NOTES AND CORRESPONDENCE

Measuring Higher-Order Moments with a Cup Anemometer

L. KRISTENSEN

Risø National Laboratory, Roskilde, Denmark

14 September 1999 and 12 December 1999

ABSTRACT

Modern, fast cup anemometers are very useful for measuring the mean-wind speed. The calibration is linear and its operation is well described as a linear, first-order filter. Discussion in the literature about the importance of the response asymmetry to increases and decreases in the streamwise turbulent wind-velocity component seems to have ended at the conclusion that there is no detectable influence on the mean-wind determination from this source, that is, the part of ‘‘overspeeding’’ due to response asymmetry can be neglected. However, a bias on the mean-wind speed from wind-direction fluctuations cannot always be excluded. Here the author addresses the problem of whether higher-order moments are influenced by the asymmetry and the direction fluctuations. Based on a theoretical analysis—a straightforward perturbation calculation—and an experimental test, the author finds that moments up to and including the fourth order are unaffected by the asymmetry as well as wind-direction fluctuations. The author suspects that this is true even for higher-order moments. It is argued that the cup anemometer together with a wind vane is well suited for measuring the horizontal components of the turbulent wind velocity.

1. Introduction

The cup anemometer was invented in 1846 by the Irish astronomer T. R. Robinson, and quite an abundance of literature has been produced about this instrument, which today has essentially the same design. Its history has been told in much detail by Middleton (1969), Kaganov and Yaglom (1976), and Wyngaard (1981), and in abbreviated forms by Kristensen (1998, 1999a,b). In the last three articles it is pointed out that the linearity of the calibration, the robustness, and the omnidirectionality make the cup anemometer well suited for routine measurements and that the so-called overspeeding is unimportant, in contrast to a rather well-established prejudice.

The speculation has been that overspeeding, which is a positive bias of the mean-wind determination, has its cause in the circumstance that the cup anemometer responds more readily to an increase than to a decrease of the wind speed and thus ‘‘spends more time on the high side than on the low side of the mean wind’’ (Kristensen 1993). In fact, if there is a bias it is caused almost entirely by wind-direction fluctuations and not by the asymmetric response.

Corresponding author address: Dr. Leif Kristensen, Risø National Laboratory, Wind Energy and Atmospheric Physics Department Building 125, P.O. Box 49, DK-4000 Roskilde, Denmark.
E-mail: leif.kristensen@risoe.dk

But what about higher-order moments? Frenzen (1988) showed that it is possible to construct a cup anemometer with a distance constant as small as 0.2 m, which means that it can easily compete with the sonic anemometer in resolving the smallest turbulent eddies of the streamwise velocity component. Will the asymmetric response or the wind-direction fluctuations give rise to a bias of the determination of second-, third-, and fourth-order moments? This is the subject of the following analysis.

2. Theoretical considerations

The equation of motion for the cup rotor can be written

$$\dot{\tilde{s}} = F(\tilde{s}, \tilde{h}, \tilde{w}), \tag{1}$$

where $\tilde{s}$ is the instantaneous angular velocity of the rotor,

$$\tilde{h} = (\tilde{u}^2 + \tilde{v}^2)^{1/2}, \tag{2}$$

the instantaneous horizontal wind velocity with the $\tilde{u}$ component along and $\tilde{v}$ perpendicular to the mean-wind direction, and $\tilde{w}$ the instantaneous vertical velocity component. Equation (1) states that the rate of change of $\tilde{s}$ is a function F of the wind velocity and angular velocity itself.

Kristensen (1998) expanded (1) to second order in $(\tilde{s}, \tilde{u}, \tilde{v}, \tilde{w})$ in the neighborhood of the mean-wind velocity $U \equiv \langle \tilde{u} \rangle$ and the cup anemometer response S to a *constant, horizontal* wind velocity with the magnitude U. Expressed in terms of the relative fluctuations

$$s = \frac{\tilde{s} - S}{S}, \tag{3}$$

$$u = \frac{\tilde{u} - U}{U}, \tag{4}$$

$$\upsilon = \frac{\tilde{\upsilon}}{U}, \quad \text{and} \tag{5}$$

$$w = \frac{\tilde{w}}{U}, \tag{6}$$

the result was

$$\tau_0 \dot{s} + s = a_1 u + a_2 w + a_3 s^2 + a_4 u^2 + a_5 w^2 + a_6 su + a_7 uw + a_8 ws + \frac{1}{2}\upsilon^2 + O(\eta^3), \tag{7}$$

where τ_0 is the instrument time constant, which is inversely proportional to U, and $a_1, \ldots, a_8$ are dimensionless constants. The last term is the third-order residual with $\eta = \max(|u|, |\upsilon|, |w|)$. Apart from the term $\frac{1}{2}\upsilon^2$, this is exactly the equation Wyngaard et al. (1974) suggested for describing the dynamical behavior of the cup anemometer.

Kristensen (1998) constructed a phenomenological model for the cup equation of motion in terms of five instruments constants and interpreted the coefficients $a_1, \ldots, a_8$.

In the following we shall simplify the discussion a little and assume that S is proportional to U and that the anemometer has an ideal angular response, that is, that it is insensitive to w. The implications are

$$a_1 = 1, \tag{8}$$

$$a_2 = a_5 = a_7 = a_8 = 0, \quad \text{and} \tag{9}$$

$$a_3 + a_4 + a_6 = 0. \tag{10}$$

On the basis of (8) and (9), (7) reduces to

$$\tau_0 \dot{s} + s = u + a_3 s^2 + a_4 u^2 + a_6 us + \frac{\upsilon^2}{2} + O(\eta^3) \tag{11}$$

with the constraint (10).

Even truncated after second order, this equation cannot in general be solved analytically with specified external forcing functions $u(t)$ and $\upsilon(t)$. However, under the rather realistic assumption that the variances of s, u, and υ are less than one, we may obtain an approximate solution by means of a perturbation calculation.

a. Perturbation scheme

We follow a standard procedure and write the solution in the form

$$s = \sum_{\ell=1}^{\infty} s_\ell, \qquad s_\ell = O(\eta^\ell). \tag{12}$$

This of course leads to an infinite hierarchy of equations. In the following we need only the first two and they are

$$\tau_0 \dot{s}_1 + s_1 = u \quad \text{and} \tag{13}$$

$$\tau_0 \dot{s}_2 + s_2 = a_3 s_1^2 + a_4 u^2 + a_6 us_1 + \frac{\upsilon^2}{2}. \tag{14}$$

Solving (13) and (14), we get

$$s_1(t) = \int_0^\infty e^{-t_1/\tau_0} \frac{dt_1}{\tau_0} u(t - t_1) \quad \text{and} \tag{15}$$

$$\begin{aligned} s_2(t) = {} & a_3 \int_0^\infty e^{-t_1/\tau_0} \frac{dt_1}{\tau_0} s_1^2(t - t_1) \\ & + a_4 \int_0^\infty e^{-t_1/\tau_0} \frac{dt_1}{\tau_0} u^2(t - t_1) \\ & + a_6 \int_0^\infty e^{-t_1/\tau_0} \frac{dt_1}{\tau_0} u(t - t_1) s_1(t - t_1) \\ & + \frac{1}{2} \int_0^\infty e^{-t_1/\tau_0} \frac{dt_1}{\tau_0} \upsilon^2(t - t_1). \end{aligned} \tag{16}$$

We now determine the mean $\mathcal{M}_1 = \langle s \rangle$ and the central moments $\mathcal{M}_\ell = \langle (s - \langle s \rangle)^\ell \rangle$ for $\ell > 1$, under the assumption that s and the wind components are stationary time series. Mean values, indicated by angle brackets $\langle\ \rangle$, are here to be understood as ensemble averages. This means that all moments are independent of time and that averages of products of the random variables at different times are functions only of the *time differences*, not of absolute time.

The expressions for $\mathcal{M}_\ell$ are truncated after the $\ell + 1$'s order. First, however, we derive a few simple relations from (13) and (14) without referring directly to the explicit solution (15) and (16).

Multiplying (13) by $s_1^{\ell-1}$, where ℓ is an integer greater than zero, and averaging, we get

$$\underbrace{\frac{\tau_0}{\ell} \frac{d}{dt} \langle s_1^\ell \rangle}_{=0} + \langle s_1^\ell \rangle = \langle u s_1^{\ell-1} \rangle \Rightarrow \langle s_1^\ell \rangle = \langle u s_1^{\ell-1} \rangle, \qquad \ell \ge 1, \tag{17}$$

since $s_1(t)$ and any power of $s_1(t)$ are stationary.

Next, we multiply (13) by $(\ell - 1)s_1^{\ell-2}s_2$ and (14) by $s_1^{\ell-1}$ ($\ell \ge 1$), add the two equations, and average. The result is

$$\ell \langle s_1^{\ell-1} s_2 \rangle = (\ell - 1)\langle u s_1^{\ell-2} s_2 \rangle + a_3 \langle s_1^{\ell+1} \rangle + a_4 \langle u^2 s_1^{\ell-1} \rangle + a_6 \langle u s_1^\ell \rangle + \frac{\langle \upsilon^2 s_1^{\ell-1} \rangle}{2}. \tag{18}$$

Using (17) to obtain

$$\langle s_1^{\ell+1}\rangle = \langle u s_1^{\ell}\rangle, \qquad (19)$$

we may, by means of the constraint (10), reformulate (18) as

$$\ell\langle s_1^{\ell-1}s_2\rangle = (\ell - 1)\langle u s_1^{\ell-2}s_2\rangle + a_4\{\langle u^2 s_1^{\ell-1}\rangle - \langle u s_1^{\ell}\rangle\} + \frac{\langle v^2 s_1^{\ell-1}\rangle}{2}, \qquad \ell \geq 1. \qquad (20)$$

Now we derive the moments. The first moment, also called the overspeeding, becomes

$$\mathcal{M}_1 = \underbrace{\langle s_1\rangle}_{=0} + \langle s_2\rangle + O(\eta^3). \qquad (21)$$

By setting $\ell = 1$ in (17) it is easily seen that the first term is zero. This is so because $\langle u\rangle = 0$ according to the definition (4).

We find $\langle s_2\rangle$ by setting $\ell = 1$ in (20) and consequently,

$$\mathcal{M}_1 = a_4(\langle u^2\rangle - \langle u s_1\rangle) + \frac{\langle v^2\rangle}{2} + O(\eta^3). \qquad (22)$$

This is the simplest expression for the overspeeding. The first of the three terms on the right-hand side corresponds to a high-pass filtering of the streamwise velocity component and the second to the systematic error due to wind-direction fluctuations. This second term dominates. A detailed discussion of overspeeding has been carried out by Kristensen (1998).

For $\ell \geq 2$ we have

$$\begin{aligned}\mathcal{M}_\ell &= \langle\{s - \langle s\rangle\}^\ell\rangle \\ &= \langle\{(s_1 + s_2 + s_3 + \cdots) - (\langle s_2\rangle + \langle s_3\rangle + \cdots)\}^\ell\rangle \\ &= \langle s_1^\ell\rangle + \ell\langle s_1^{\ell-1}s_2\rangle - \ell\langle s_1^{\ell-1}\rangle\langle s_2\rangle + O(\eta^{\ell+2}). \qquad (23)\end{aligned}$$

Applying the relations (17) and (20), we obtain

$$\begin{aligned}\mathcal{M}_\ell = {} & \underbrace{\langle s_1^\ell\rangle}_{O(\eta^\ell)} + (\ell - 1)\underbrace{\langle u s_1^{\ell-2}s_2\rangle}_{O(\eta^{\ell+1})} \\ & + a_4\{\underbrace{\langle u^2 s_1^{\ell-1}\rangle}_{O(\eta^{\ell+1})} - \underbrace{\langle u s_1^\ell\rangle}_{O(\eta^{\ell+1})} - \ell\underbrace{\langle u s_1^{\ell-2}\rangle[\langle u^2\rangle - \langle u s_1\rangle]}_{O(\eta^{\ell+1})}\} \\ & + \frac{1}{2}\underbrace{\langle v^2 s_1^{\ell-1}\rangle}_{O(\eta^{\ell+1})} - \frac{\ell}{2}\underbrace{\langle v^2\rangle\langle u s_1^{\ell-2}\rangle}_{O(\eta^{\ell+1})} + O(\eta^{\ell+2}). \qquad (24)\end{aligned}$$

This is as far as we can reduce the expressions for the moments without actually solving (13) and (14) and using (15) and (16).

We note that for $\ell \geq 2$, the leading term in the expression for $\mathcal{M}_\ell$ is $\langle s_1^\ell\rangle$. According to (13), $s_1(t)$ is the response of a linear, first-order filter to the input $u(t)$. This means that if the instrument reacts fast enough to resolve the smallest eddies (τ_0 small), the leading term in each of the central moments $\mathcal{M}_\ell$ are actually the corresponding moments of u.

The important question is, therefore, if the next term in $\mathcal{M}_\ell$, which is of order $\ell + 1$ in η, will be detectable compared to the first in magnitude. If this is the case there will be a bias in higher-order moments when they are determined by a cup anemometer. If not, a fast cup anemometer will be well suited for measuring higher-order moments of the fluctuating, streamwise velocity component.

Consequently, we define the residuals

$$\delta\mathcal{M}_\ell \equiv \mathcal{M}_\ell - \langle s_1^\ell\rangle, \qquad \ell \geq 2. \qquad (25)$$

Since they are all of higher order than two, we must use approximations to reduce them to moments of order two or less.

b. Approximations

We will make the simplest possible approximation, namely, that $u(t)$ is a Gaussian process. Since any linear combination of $u(t)$'s, taken at different times t, is also Gaussian, it follows from (15) and (16) that $s_1(t)$ and $s_2(t)$ are also Gaussian processes.

For Gaussian processes with zero means all odd moments are zero and all even moments can be reduced to homogeneous polynomials in second-order moments by means of the Isserlis relation (an elegant proof can be found in Frisch 1995). From now we limit ourselves to cases where $\ell \leq 4$ and all we need here is the reduction of fourth-order moments, for which

$$\langle x_1x_2x_3x_4\rangle = \langle x_1x_2\rangle\langle x_3x_4\rangle + \langle x_1x_3\rangle\langle x_2x_4\rangle + \langle x_1x_4\rangle\langle x_2x_3\rangle \qquad (26)$$

for four joint-Gaussian random variables (x_1, x_2, x_3, x_4) with zero means.

The first implications are

$$\delta\mathcal{M}_2 = O(\eta^4) \quad \text{and} \qquad (27)$$

$$\delta\mathcal{M}_4 = O(\eta^6). \qquad (28)$$

We will need to work a little harder on

$$\begin{aligned}\delta\mathcal{M}_3 = {} & 2\langle u s_1 s_2\rangle \\ & + a_4\{\langle u^2 s_1^2\rangle - \langle u s_1^3\rangle - 3\langle u s_1\rangle[\langle u^2\rangle - \langle u s_1\rangle]\} \\ & + \frac{\langle v^2 s_1^2\rangle}{2} - \frac{3}{2}\langle v^2\rangle\langle u s_1\rangle + O(\eta^5). \qquad (29)\end{aligned}$$

By means of the Isserlis relation and (19) we can simplify (29) somewhat. We have

$$\langle u^2 s_1^2\rangle = \langle u^2\rangle\langle s_1^2\rangle + 2\langle u s_1\rangle^2 = \langle u^2\rangle\langle u s_1\rangle + 2\langle u s_1\rangle^2, \qquad (30)$$

$$\langle u s_1^3\rangle = 3\langle u s_1\rangle\langle s_1^2\rangle = 3\langle u s_1\rangle^2, \quad \text{and} \qquad (31)$$

$$\begin{aligned}\langle v^2 s_1^2\rangle &= \langle v^2\rangle\langle s_1^2\rangle + 2\langle v s_1\rangle^2 = \langle v^2\rangle\langle u s_1\rangle + 2\langle v s_1\rangle^2 \\ &= \langle v^2\rangle\langle u s_1\rangle, \qquad (32)\end{aligned}$$

since, in view of (15) and Taylor's hypothesis, $\langle v(t)s_1(t)\rangle$ must be zero due to reflection symmetry.

The expression for $\delta\mathcal{M}_3$ reduces to

$$\delta\mathcal{M}_3 = 2\{\langle u s_1 s_2\rangle - a_4\langle u s_1\rangle[\langle u^2\rangle - \langle u s_1\rangle]\} - \langle v^2\rangle\langle u s_1\rangle + O(\eta^5). \qquad (33)$$

We can break down (33) even further by using (15), (16), and the Isserlis relation on $\langle u s_1 s_2\rangle$:

$$
\begin{aligned}
\langle us_1s_2\rangle &= \langle u(t)s_1(t)s_2(t)\rangle = a_3\int_0^\infty e^{-t_1/\tau_0}\,\frac{dt_1}{\tau_0}\langle u(t)s_1(t)s_1^2(t-t_1)\rangle + a_4\int_0^\infty e^{-t_1/\tau_0}\,\frac{dt_1}{\tau_0}\,\langle u(t)s_1(t)u^2(t-t_1)\rangle \\
&\quad + a_6\int_0^\infty e^{-t_1/\tau_0}\,\frac{dt_1}{\tau_0}\langle u(t)s_1(t)u(t-t_1)s_1(t-t_1)\rangle + \frac{1}{2}\int_0^\infty e^{-t_1/\tau_0}\,\frac{dt_1}{\tau_0}\langle u(t)s_1(t)v^2(t-t_1)\rangle \\
&= a_3\left\{\langle us_1\rangle\langle s_1^2\rangle + 2\int_0^\infty e^{-t_1/\tau_0}\,\frac{dt_1}{\tau_0}\langle u(t)s_1(t-t_1)\rangle\langle s_1(t)s_1(t-t_1)\rangle\right\} \\
&\quad + a_4\left\{\langle us_1\rangle\langle u^2\rangle + 2\int_0^\infty e^{-t_1/\tau_0}\,\frac{dt_1}{\tau_0}\langle u(t)u(t-t_1)\rangle\langle s_1(t)u(t-t_1)\rangle\right\} \\
&\quad + a_6\left\{\langle us_1\rangle^2 + \int_0^\infty e^{-t_1/\tau_0}\,\frac{dt_1}{\tau_0}\langle u(t)u(t-t_1)\rangle\langle s_1(t)s_1(t-t_1)\rangle + \int_0^\infty e^{-t_1/\tau_0}\,\frac{dt_1}{\tau_0}\langle u(t)s_1(t-t_1)\rangle\langle s_1(t)u(t-t_1)\rangle\right\} \\
&\quad + \frac{1}{2}\left\{\langle us_1\rangle\langle v^2\rangle + 2\int_0^\infty e^{-t_1/\tau_0}\,\frac{dt_1}{\tau_0}\underbrace{\langle u(t)v(t-t_1)\rangle}_{=0}\langle s_1(t)v(t-t_1)\rangle\right\} \\
&= a_4\langle us_1\rangle\{\langle u^2\rangle - \langle us_1\rangle\} + \frac{1}{2}\langle us_1\rangle\langle v^2\rangle + 2a_3\int_0^\infty e^{-t_1/\tau_0}\,\frac{dt_1}{\tau_0}\langle u(t)s_1(t-t_1)\rangle\langle s_1(t)s_1(t-t_1)\rangle \\
&\quad + 2a_4\int_0^\infty e^{-t_1/\tau_0}\,\frac{dt_1}{\tau_0}\langle u(t)u(t-t_1)\rangle\langle s_1(t)u(t-t_1)\rangle + a_6\int_0^\infty e^{-t_1/\tau_0}\,\frac{dt_1}{\tau_0}\langle u(t)u(t-t_1)\rangle\langle s_1(t)s_1(t-t_1)\rangle \\
&\quad + a_6\int_0^\infty e^{-t_1/\tau_0}\,\frac{dt_1}{\tau_0}\langle u(t)s_1(t-t_1)\rangle\langle s_1(t)u(t-t_1)\rangle. \qquad (34)
\end{aligned}
$$

There are four types of covariances: $\langle u(t)u(t-t_1)\rangle$, $\langle u(t)s_1(t-t_1)\rangle$, $\langle s_1(t)u(t-t_1)\rangle$, and $\langle s_1(t)s_1(t-t_1)\rangle$. Since $u(t)$ and $s_1(t)$ are stationary these covariances are independent of absolute time t. We have

$$\langle u(t)u(t-t_1)\rangle = R(t_1), \qquad (35)$$

where $R(t)$ is the autocovariance function. It then follows from (15) that

$$\langle u(t)s_1(t-t_1)\rangle = \int_0^\infty e^{-t_2/\tau_0}\,\frac{dt_2}{\tau_0}R(t_1+t_2), \qquad (36)$$

$$\langle s_1(t)u(t-t_1)\rangle = \int_0^\infty e^{-t_2/\tau_0}\,\frac{dt_2}{\tau_0}R(t_2-t_1), \quad \text{and} \qquad (37)$$

$$
\begin{aligned}
\langle s_1(t)s_1(t-t_1)\rangle &= \int_0^\infty e^{-t_2/\tau_0}\,\frac{dt_2}{\tau_0}\int_0^\infty e^{-t_3/\tau_0}\,\frac{dt_3}{\tau_0} \\
&\quad \times R(t_1+t_3-t_2) \\
&= \frac{1}{2}\int_0^\infty e^{-t_2/\tau_0}\,\frac{dt_2}{\tau_0} \\
&\quad \times \{R(t_1+t_2) + R(t_2-t_1)\}. \qquad (38)
\end{aligned}
$$

To show that they are all about the same when τ_0 is much smaller than the integral timescale

$$\mathcal{T} \equiv \frac{1}{\langle u^2\rangle}\int_0^\infty R(t)\,dt, \qquad (39)$$

we apply the identity

$$\int_0^\infty e^{-t/\tau_0}\,\frac{dt}{\tau_0}f(t) = \sum_{\ell=0}^\infty f^{(\ell)}(0)\tau_0^\ell, \qquad (40)$$

where $f^{(\ell)}(t)$ denotes the ℓ's derivative of the function $f(t)$.

Thus, to second order in τ_0 we get

$$\langle u(t)s_1(t-t_1)\rangle \approx R(t_1) + \dot{R}(t_1)\tau_0 + \ddot{R}(t_1)\tau_0^2, \qquad (41)$$

$$\langle s_1(t)u(t-t_1)\rangle \approx R(t_1) - \dot{R}(t_1)\tau_0 + \ddot{R}(t_1)\tau_0^2, \qquad (42)$$

and

$$\langle s_1(t)s_1(t-t_1)\rangle + R(t_1) + \ddot{R}(t_1)\tau_0^2. \qquad (43)$$

Inserting in (34), the integrals become, by applying again the identity (40),

$$\int_0^\infty e^{-t_1/\tau_0}\,\frac{dt_1}{\tau_0}\langle u(t)s_1(t-t_1)\rangle\langle s_1(t)s_1(t-t_1)\rangle \approx R^2(0) + 5R(0)\ddot{R}(0)\tau_0^2, \quad (44)$$

$$\int_0^\infty e^{-t_1/\tau_0}\,\frac{dt_1}{\tau_0}\langle u(t)u(t-t_1)\rangle\langle s_1(t)u(t-t_1)\rangle \approx R^2(0) + 2R(0)\ddot{R}(0)\tau_0^2, \quad \text{and} \quad (45)$$

$$\frac{1}{2}\int_0^\infty e^{-t_1/\tau_0}\,\frac{dt_1}{\tau_0}\{\langle u(t)u(t-t_1)\rangle\langle s_1(t)s_1(t-t_1)\rangle + \langle u(t)s_1(t-t_1)\rangle\langle s_1(t)u(t-t_1)\rangle\} \approx R^2(0) + \frac{7}{2}R(0)\ddot{R}(0)\tau_0^2. \quad (46)$$

There are no terms containing $\dot{R}(0)$ since $R(t)$ is an even function.

We now need a realistic expression for $R(t)$ when t is approaching zero. In many studies of this nature the turbulent flow is assumed to be governed by the rules of local isotropy, without being directly influenced by the viscous dissipation of the kinetic energy. We may obtain such an expression by starting from the power spectrum $S(\omega)$ since

$$R(t) = \int_{-\infty}^{\infty} S(\omega)\cos(\omega t)\,d\omega. \quad (47)$$

Accepting Taylor's hypothesis for frozen turbulence, we have for $|\omega|\mathcal{T} \gtrsim 1$

$$S(\omega) = A\langle u^2\rangle\mathcal{T}(|\omega|\mathcal{T})^{-5/3}, \quad (48)$$

where A is a dimensionless constant. This is the spectrum of u at high frequencies when observed by means of an instrument with high (but not infinite) temporal resolution. However, any instrument has a finite temporal resolution. For the cup anemometer, for example, it is necessary to average in time over at least one full revolution of the rotor since its angular velocity is quite uneven (see, e.g., Coppin 1982). For constant wind it is periodical with a period equal to the duration of one revolution that, for most cup anemometers, is not far from the time constant τ_0. Also the sonic anemometer has a finite temporal resolution since it averages the velocity field over lines of finite lengths. This general, instrumentally imposed averaging must be taken into account in the expression for $S(\omega)$ by multiplying by a transfer function corresponding to the instrumental temporal resolution. Let us here just assume that the averaging is an unweighted average over the time θ, corresponding to the cup anemometer case. Then (48) must be replaced by

$$S(\omega) = A\,\mathrm{sinc}^2\left(\frac{\theta\omega}{2}\right)\langle u^2\rangle\mathcal{T}(|\omega|\mathcal{T})^{-5/3}, \quad (49)$$

where $\mathrm{sinc}(x) = \sin(x)/x$.

The autocovariance function can now be obtained from (47) as follows:

$$R(t) = \int_{-\infty}^{\infty} S(\omega)\cos(\omega t)\,d\omega = \underbrace{\int_{-\infty}^{\infty} S(\omega)\,d\omega}_{=\langle u^2\rangle} - 2\int_0^\infty S(\omega)\{1-\cos(\omega t)\}\,d\omega$$

$$= \langle u^2\rangle\left[1 - 2A\mathcal{T}\int_0^\infty \mathrm{sinc}^2\left(\frac{\omega\theta}{2}\right)\{1-\cos(\omega t)\}(\omega\mathcal{T})^{-5/3}\,d\omega\right] = \langle u^2\rangle\left\{1 - \frac{3}{2}\Gamma\left(\frac{1}{3}\right)A\frac{t^2}{\mathcal{T}^{2/3}\theta^{4/3}} + O\left(\frac{|t|^{8/3}}{\mathcal{T}^{2/3}\theta^2}\right)\right\}. \quad (50)$$

Thus,

$$\ddot{R}(0)\tau_0^2 = R(0)O\left(\left[\frac{\tau_0}{\mathcal{T}}\right]^{2/3}\left[\frac{\tau_0}{\theta}\right]^{4/3}\right). \quad (51)$$

Substituting in (34), we get

$$\langle us_1s_2\rangle = a_4\langle us_1\rangle\{\langle u^2\rangle - \langle us_1\rangle\} + \frac{1}{2}\langle v^2\rangle\langle us_1\rangle + 2\underbrace{(a_3 + a_4 + a_6)}_{=0}R^2(0) + R^2(0)O\left(\left[\frac{\tau_0}{\mathcal{T}}\right]^{2/3}\left[\frac{\tau_0}{\theta}\right]^{4/3}\right). \quad (52)$$

The expression (33) for $\delta\mathcal{M}_3$ reduces to

$$\delta\mathcal{M}_3 = \langle u^2\rangle^2 O\left(\left[\frac{\tau_0}{\mathcal{T}}\right]^{2/3}\left[\frac{\tau_0}{\theta}\right]^{4/3}\right) + O(\eta^5). \quad (53)$$

On basis of these considerations it seems natural to postulate that the correction terms $\delta\mathcal{M}_\ell$ are very small so that the second, third, and fourth moments of the streamwise velocity component can be determined without bias by means of a cup anemometer.

3. Experimental field test

In July 1994 wind speed measurements were carried out at a height of 6 m from two masts separated by 3 m inside an artillery shooting range at Borris in Jutland in Denmark. A Solent Ultrasonic Anemometer model 1012R was mounted at the top of one mast and a cup

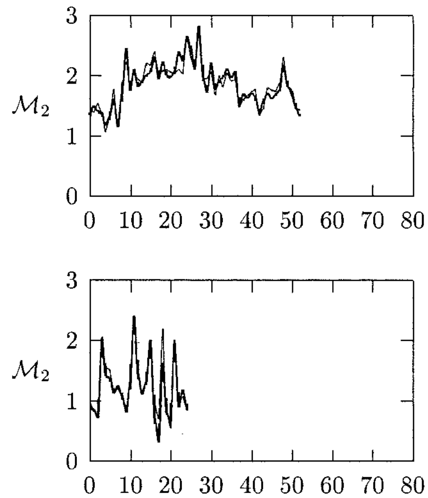

FIG. 1. Time series of second-order moments. Thick line, cup data; thin line, sonic data. The time along the abscissa is in units of 10 min.

anemometer with a distance constant l_0 equal to about 1.5 m plus a wind direction vane at the top of the other. According to, for example, Kristensen et al. (1989), the turbulence length scale $\mathcal{L}$ for the streamwise velocity component is about five times the height of observation, that is, about 30 m. This means that $\tau_0/\mathcal{T} = l_0/\mathcal{L} \approx 0.05$. The sampling rates were 10 Hz for the sonic and 5 Hz for the cup and vane. The experiment is described in detail by Kristensen (1999a). The same four periods are analyzed and the intercalibration between the sonic and the cup from these data are applied in the calculation of 10-min averages of the higher-order moments of the streamwise velocity component.

In this section u and s are the fluctuating, streamwise wind velocity component and cup anemometer output in physical units, both measured in meters per second, and the results in the form of time series are shown in Figs. 1, 2, and 3.

Apparently, the moments determined by the cup anemometer track the sonic moments in a way that seems to support our postulate that there are no systematic difference between $\langle s^l \rangle$ and $\langle u^l \rangle$.

More revealing tests are plots of $\langle s^l \rangle$ versus $\langle u^l \rangle$. Figures 4, 5, and 6 show these comparisons.

Only the linear, least squares fit to the third-order moment seems to deviate significantly from the line $\langle s^3 \rangle = \langle u^3 \rangle$. Even in this case this line seems a reasonable fit to most of the points. We have taken a closer look at the situation. Inspecting Fig. 2, we see that there is a large difference between $\langle s^3 \rangle$ and $\langle u^3 \rangle$ at one particular time in the third record in the lower left frame. The point indicated by a filled circle in Fig. 5 corresponds

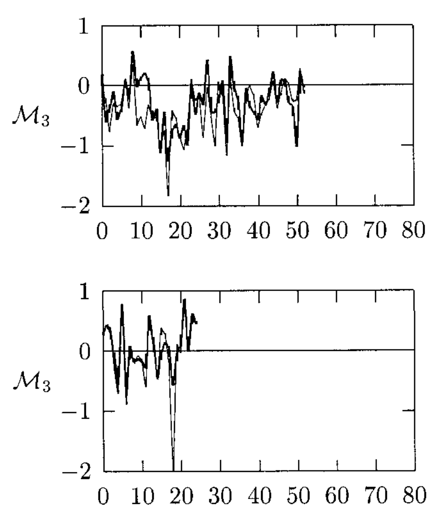

FIG. 2. Time series of third-order moments. Thick line, cup data; thin line, sonic data. The time along the abscissa is in units of 10 min.

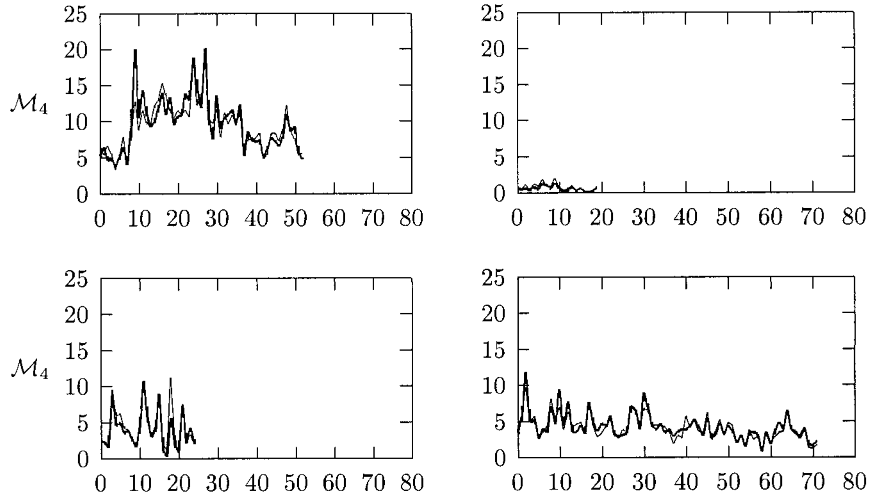

FIG. 3. Time series of fourth-order moments. Thick line, cup data; thin line, sonic data. The time along the abscissa is in units of 10 min.

to the same difference. This outlier seems to influence the slope significantly, in particular because we minimize the sum of the squares of the *vertical,* rather than the *perpendicular* distance to a straight line, thereby exaggerating the problem. We have fitted straight lines to the points once again, with and without the outlier, and this time we have used orthogonal linear regression. Actually, this is justified by the argument that $\langle s^3 \rangle$ and $\langle u^3 \rangle$, representing two independent estimates of the same quantity, should be treated statistically in a symmetric way. We find that the slope and the offset are 0.86 $\pm$ 0.08 and 0.03 $\pm$ 0.04 when the outlier is included and 0.95 $\pm$ 0.08 and 0.04 $\pm$ 0.04 when it is excluded. The number of observations is 169, which means that the standard error is $1/\sqrt{169} \simeq 0.077$. This means that the difference between the slopes divided by this standard error becomes 1.2, a number, which according to Neter et al. (1989), shows that the outlier must be considered influential. Except that the wind speed in this particular 10-min period was very instationary, it has not been possible to determine if there should be a particular physical reason for the large deviation of one point from the fitted line. However, in view of how well $\langle s^3 \rangle$ and $\langle u^3 \rangle$ otherwise track one another in Fig. 2, it seems reasonable to exclude this point from the analysis. If we do that the new fit of the slope is within one standard

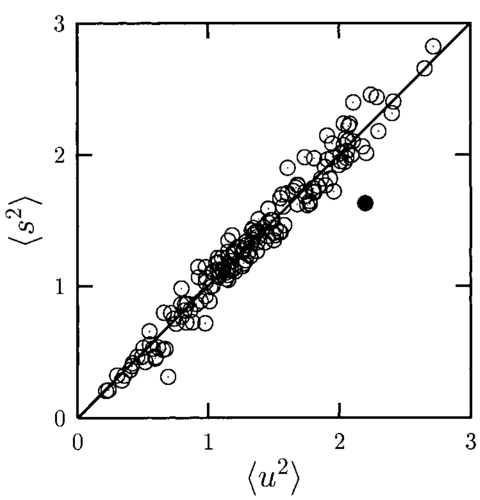

FIG. 4. Comparison between second-order moments. The thick line corresponds to $\langle s^2 \rangle = \langle u^2 \rangle$ and thin line (hardly discernable) the linear, least squares fit to all the points with equal weight, slope 1.01 $\pm$ 0.02 and offset -0.01 ± 0.02.

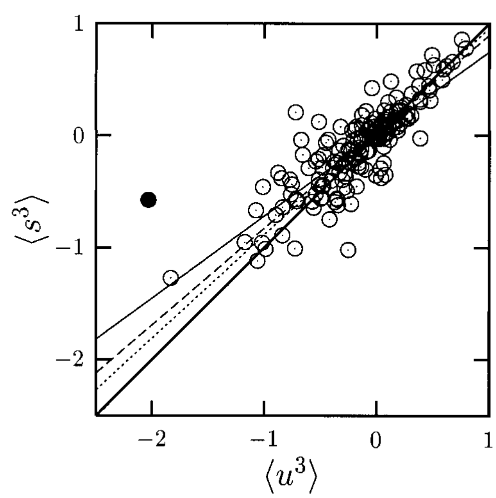

FIG. 5. Comparison between third-order moments. The thick line corresponds to $\langle s^3 \rangle = \langle u^3 \rangle$ and thin line the linear, least squares fit to all the points with equal weight, slope 0.73 $\pm$ 0.04 and offset 0.01 $\pm$ 0.02. The single outlier, which can also be seen in the lower left frame of Fig. 2, is marked with a filled circle. The dashed and the dotted line are orthogonal linear regression lines to the measurements, with and without the outlier, respectively. The first has the slope 0.86 $\pm$ 0.08 and the offset 0.03 $\pm$ 0.04; the second, 0.95 $\pm$ 0.08 and 0.04 $\pm$ 0.04.

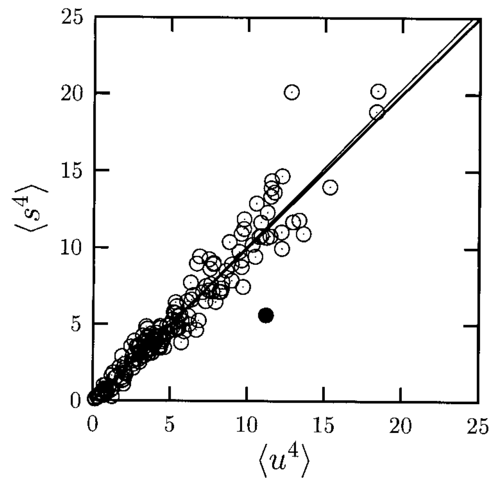

FIG. 6. Comparison between fourth-order moments. The thick line corresponds to $\langle s^4\rangle = \langle u^4\rangle$ and thin line the linear, least squares fit to all the points with equal weight, slope 1.02 $\pm$ 0.02 and offset -0.12 ± 0.16.

error of 1. In Figs. 4 and 6 the second- and fourth-order moments from this period of observation are indicated by filled circles. In these cases the outliers do not seem to influence the least squares fits significantly, in the first case probably because lower-order moments are less sensitive, and in the second because the range of fourth-order moments is very large.

Taking a closer look at the longest record, which is displayed in the fourth frame of Figs. 1, 2, and 3, we may present the data in still another form, namely, as histograms of $\langle u^l\rangle$, $\langle s^l\rangle$, and $\langle s\rangle^l - \langle u\rangle^l$. This record contains a total number of 72 observations and the histograms are displayed in Figs. 7, 8, 9, with the means and root-mean-square (rms) deviations summarized in Table 1.

Inspecting Figs. 7, 8, 9, and Table 1, we note

1) that systematic differences between the means and root-mean-square deviations of $\langle u^l\rangle$ and $\langle s^l\rangle$ are undetectable;

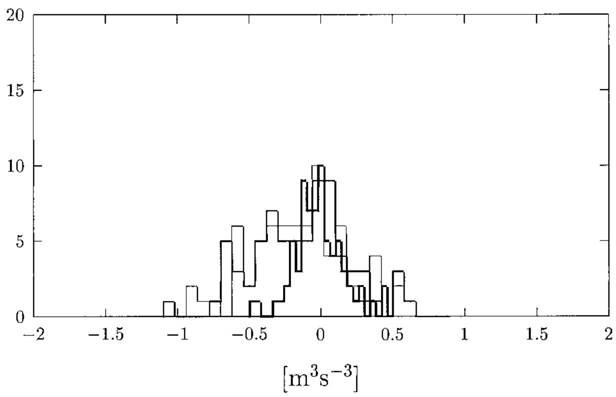

FIG. 8. Histograms of $\langle u^3\rangle$ (thin line), $\langle s^3\rangle$ (thicker line), and $\langle s^3\rangle - \langle u^3\rangle$ (thick line).

2) that the means of $\langle s^l\rangle - \langle u^l\rangle$ are between 3 and 8 times smaller than their root-mean-square deviations, and between 10 and 18 times smaller than the root-mean-square deviations of $\langle u^l\rangle$ and $\langle s^l\rangle$; and
3) that the root-mean-square deviations of $\langle s^l\rangle - \langle u^l\rangle$ are between 2 and 3 times smaller than those of $\langle u^l\rangle$ and $\langle s^l\rangle$.

With respect to item 2 one could, on the basis of Table 1, argue that, with as many as 72 observations, the means of $\langle s^l\rangle - \langle u^l\rangle$ might be slightly positive, that is, that the cup anemometer will overestimate higher-order moments compared to the sonic anemometer. However, in view of item 3, these ''systematic errors'' are, if existing, so small that they are of no importance from a field experimental point of view.

We may also compare the skewness

$$\mathcal{S} = \frac{\mathcal{M}_3}{\langle s^2\rangle^{3/2}} \tag{54}$$

and the kurtosis

$$\mathcal{K} = \frac{\mathcal{M}_4}{\langle s^2\rangle^2} \tag{55}$$

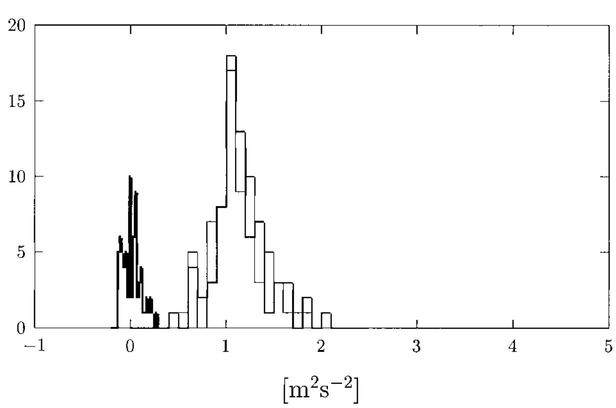

FIG. 7. Histograms of $\langle u^2\rangle$ (thin line), $\langle s^2\rangle$ (thicker line), and $\langle s^2\rangle - \langle u^2\rangle$ (thick line).

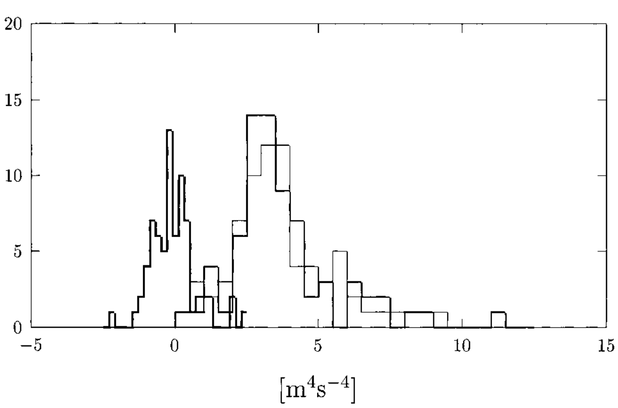

FIG. 9. Histograms of $\langle u^4\rangle$ (thin line), $\langle s^4\rangle$ (thicker line), and $\langle s^4\rangle - \langle u^4\rangle$ (thick line).

TABLE 1. Means and root-mean-square deviations of $\langle u^\ell \rangle$, $\langle s^\ell \rangle$, and $\langle s^\ell \rangle - \langle u^\ell \rangle$.

	Mean	rms
$\langle u^2 \rangle$	1.209	0.272
$\langle s^2 \rangle$	1.240	0.288
$\langle s^2 \rangle - \langle u^2 \rangle$	0.031	0.097
$\langle u^3 \rangle$	−0.083	0.352
$\langle s^3 \rangle$	−0.062	0.342
$\langle s^3 \rangle - \langle u^3 \rangle$	0.021	0.172
$\langle u^4 \rangle$	4.125	1.696
$\langle s^4 \rangle$	4.244	1.896
$\langle s^4 \rangle - \langle u^4 \rangle$	0.119	0.764

determined by means of the cup anemometer with those obtained by means of the sonic. These comparisons are shown in Figs. 10 and 11. Both ordinary least squares fit and orthogonal linear regression has been applied to the data points in these figures.

Again the identity lines seem to be consistent with data.

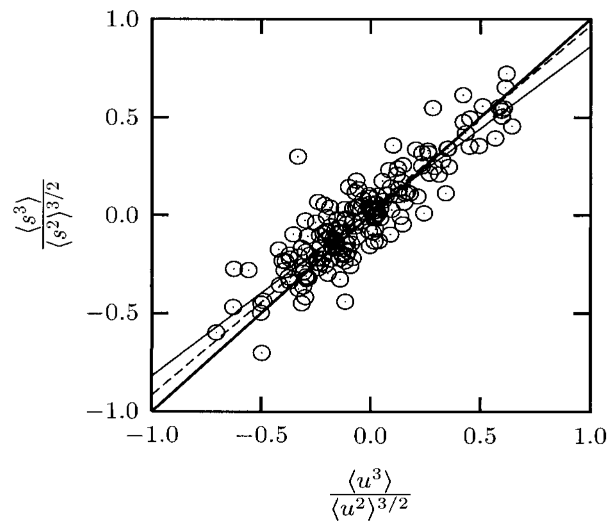

FIG. 10. Comparison between the skewnesses. The thick line corresponds to identity and the thin line to a linear, least squares fit with equal weight to each point, slope 0.84 ± 0.03 and offset 0.02 ± 0.01. The orthogonal linear regression, shown by a dashed line, has slope 0.94 ± 0.08 and offset 0.03 ± 0.030.

4. Conclusions

The theoretical analysis of higher-order moments, including the fourth order, of the cup anemometer signal has shown that these, to a high degree of accuracy, should be indistinguishable from the moment of the true streamwise velocity component as observed through a first-order, linear filter with the time constant τ_0, characterizing the response of the anemometer (at one particular mean wind velocity). A comparison with a sonic signal seems to confirm this prediction.

In retrospect this is really not surprising. We know from previous analyses (Kristensen 1998, 1999b) that the asymmetric cup anemometer response is probably unimportant for the overspeeding and that the mean of the cup anemometer signal deviates from the magnitude of the mean-wind vector by an amount that corresponds to the difference between the distance an air particle would travel along its path and the resulting distance if, during the averaging time, the wind speed at any time were the same in all points. Usually, this difference is smaller than a few percent and it goes to zero when the averaging time goes to zero. But the higher-order moments just represent identical, ''instantaneous'' fluctuations around means that are almost the same. Consequently, we should not expect that higher-order moments, not even higher than the fourth, to be affected by wind direction fluctuations. Of course, nobody would dare to make predictions on basis of these last qualitative considerations. We had to go through the painstaking analysis to feel confident with this conjecture.

It might seem that there is little motivation for attacking this particular problem of studying higher-order moments with a cup anemometer that, traditionally, is mostly used for determining the mean-wind speed. However, the results presented here show that the cup anemometer may very well serve as an instrument for studying the more detailed structure of atmospheric flows, that is, the turbulence. Compared to the sonic anemometer it has the advantage that it is omnidirectional where the sonic has a very pronounced directionality. Usually the filtering properties of the sonic anemometer are very complicated whereas the cup anemometer, with its velocity-independent distance constant, filters the flow along a line in the instantaneous

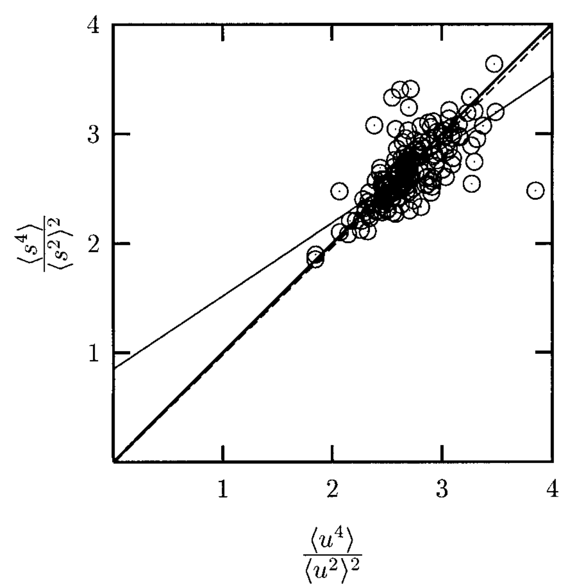

FIG. 11. Comparison between the kurtosises. The thick line corresponds to identity and the thin line to a linear, least squares fit with equal weight to each point, slope 0.67 ± 0.06 and offset 0.85 ± 0.15. The orthogonal linear regression, shown by a dashed line, has slope 0.99 ± 0.08 and offset −0.01 ± 0.21.

flow direction. Using the results of Kristensen (1998), it is easily seen that a combination of a cup anemometer and a wind vane, aligned vertically with one another, can be used to measure and resolve the horizontal velocity components of the turbulent wind field with a spatial resolution equal to the distance constant. It is accomplished by recording consecutively the duration of each cup revolution and, at the same time, the instantaneous wind direction. We see that the filtering is spatial rather than temporal. This instrument combination can be augmented by a single-component sonic anemometer, with its axis aligned with the cup–vane combination, to include the measurement of the vertical velocity component. At the end of each rotation period of the cup rotor the signal from the sonic anemometer should also be recorded and a suitable digital signal processing applied to obtain the same first-order filtering for all three instruments. The combined instrument is omnidirectional and from that point of view superior to the sonic anemometer. The spatial measuring domains of the three instruments are vertically displaced about 0.5 m with respect to each other, but as long as the scale of the turbulence is large compared to the displacements this is of little consequence when measuring momentum fluxes. The idea of combining cup, vane, and single-component sonic has apparently never been suggested in the literature, although it appears that the instrumental axisymmetry and minimal flow distortion would be significant advantages when comparing to the usual three-component sonic anemometer.

Acknowledgments. This work has been carried out under contract with the Danish Energy Agency, Project EFP-98 1363/97-0032. My colleagues Morten Nielsen, Jakob Mann, and Peter Kirkegaard, all of Risø National Laboratory, have offered useful comments and, thanks to their efforts and those of the referees, errors have been corrected and unfortunate formulations changed.

REFERENCES

Coppin, P. A., 1982: Cup anemometer overspeeding. *Meteor. Rundsch.* **35,** 1–11.

Frenzen, P., 1988: Fast response cup anemometers for atmospheric turbulence research. *Proc. Eighth Symp. on Turbulence and Diffusion,* San Diego, CA, Amer. Meteor. Soc., 112–115.

Frisch, U., 1995: *Turbulence, the Legacy of A. N. Kolmogorov.* Cambridge University Press, 296 pp.

Kaganov, E. I., and A. M. Yaglom, 1976: Errors in wind speed measurements by rotation anemometers. *Bound.-Layer Meteor.,* **10,** 1–11.

Kristensen, L., 1993: The cup anemometer and other exciting instruments. Riso National Laboratory Report Riso-R-615(EN), 82 pp.

——, 1998: Cup anemometer behavior in turbulent environments. *J. Atmos. Oceanic Technol.,* **15,** 5–17.

——, 1999a: Kopanemometret. *Vejret,* **78,** 29–40.

——, 1999b: The perennial cup anemometer. *Wind Energy,* **2,** 59–75.

——, D. H. Lenschow, P. Kirkegaard, and M. S. Courtney, 1989: The spectral velocity tensor for homogeneous boundary-layer turbulence. *Bound.-Layer Meteor.,* **47,** 149–193.

Middleton, W. E. K., 1969: *Invention of Meteorological Instruments.* The Johns Hopkins Press, 362 pp.

Neter, J., W. Wasserman, and M. H. Kutner, 1989: *Applied Linear Regression Models.* Irwin, 667 pp.

Wyngaard, J. C., 1981: Cup, propeller, vane, and sonic anemometers in turbulence research. *Ann. Rev. Fluid Mech.,* **13,** 399–423.

——, J. T. Bauman, and R. A. Lynch, 1974: Cup anemometer dynamics. *Proc. Symp. on Flow: Its Measurements and Control in Science and Industry, Vol. 1,* Pittsburg, PA, Instrument Society of America, 701–708.